

Epoxy metabolites of docosahexaenoic acid (DHA) inhibit angiogenesis, tumor growth, and metastasis

Guodong Zhang^{a,b}, Dipak Panigrahy^{c,d}, Lisa M. Mahakian^e, Jun Yang^{a,b}, Jun-Yan Liu^{a,b}, Kin Sing Stephen Lee^{a,b}, Hiromi I. Wettersten^f, Arzu Ulu^{a,b}, Xiaowen Hu^e, Sarah Tam^e, Sung Hee Hwang^{a,b}, Elizabeth S. Ingham^e, Mark W. Kieran^{c,g}, Robert H. Weiss^{b,f,h}, Katherine W. Ferrara^e, and Bruce D. Hammock^{a,b,1}

^aDepartment of Entomology, and ^bComprehensive Cancer Center, University of California, Davis, CA 95616; ^cVascular Biology Program, Children's Hospital Boston, and ^dDepartment of Pathology, Beth Israel Deaconess Medical Center, Harvard Medical School, Boston, MA 02115; ^eDepartment of Biomedical Engineering, and ^fDivision of Nephrology, Department of Internal Medicine, University of California, Davis, CA 95616; ^gDivision of Pediatric Oncology, Dana-Farber Cancer Institute, Harvard Medical School, Boston, MA 02115; and ^hUS Department of Veteran's Affairs Medical Center, Sacramento, CA 95655

Contributed by Bruce D. Hammock, March 8, 2013 (sent for review December 24, 2012)

Epidemiological and preclinical evidence supports that omega-3 dietary fatty acids (fish oil) reduce the risks of macular degeneration and cancers, but the mechanisms by which these omega-3 lipids inhibit angiogenesis and tumorigenesis are poorly understood. Here we show that epoxydocosapentaenoic acids (EDPs), which are lipid mediators produced by cytochrome P450 epoxygenases from omega-3 fatty acid docosahexaenoic acid, inhibit VEGF- and fibroblast growth factor 2-induced angiogenesis in vivo, and suppress endothelial cell migration and protease production in vitro via a VEGF receptor 2-dependent mechanism. When EDPs (0.05 mg·kg⁻¹·d⁻¹) are coadministered with a low-dose soluble epoxide hydrolase inhibitor, EDPs are stabilized in circulation, causing ~70% inhibition of primary tumor growth and metastasis. Contrary to the effects of EDPs, the corresponding metabolites derived from omega-6 arachidonic acid, epoxyeicosatrienoic acids, increase angiogenesis and tumor progression. These results designate epoxyeicosatrienoic acids and EDPs as unique endogenous mediators of an angiogenic switch to regulate tumorigenesis and implicate a unique mechanistic linkage between omega-3 and omega-6 fatty acids and cancers.

Epidemiological and preclinical evidence supports that a diet rich in omega-3 dietary fatty acids is correlated with reduced risks of angiogenic diseases such as macular degeneration (1–4) and cancers (5–8). However, the mechanisms by which omega-3 fatty acids inhibit angiogenesis and cancer are poorly understood. A widely accepted theory to explain the health-promoting effects of omega-3 fatty acids is that they suppress the metabolism of omega-6 arachidonic acid (ARA) to form proangiogenic or proinflammatory eicosanoids or serve as alternative substrates to generate omega-3 lipid mediators with beneficial actions (9). Indeed, the metabolism of omega-3 fatty acids by cyclooxygenase (COX) and lipoxygenase (LOX) enzymes generates 3-series prostaglandins (10, 11) and leukotrienes (12), as well as unique omega-3 autacoids such as resolvins and protectins (13), which have anti-inflammatory or antiangiogenic effects.

Besides the intensively studied COX and LOX pathways, omega-3 and omega-6 fatty acids are also substrates of cytochrome P450 (CYP) epoxygenases, which convert them to epoxy signaling lipids including epoxyeicosatrienoic acids (EETs) derived from omega-6 ARA and epoxydocosapentaenoic acids (EDPs) from omega-3 docosahexaenoic acid (DHA) (14–16). DHA, which is the most abundant omega-3 fatty acid in most tissues (17, 18), can efficiently compete with ARA for the metabolism by CYP epoxygenases, leading to replacement of EETs with EDPs in vivo (16, 19, 20). EETs and EDPs have been investigated as autocrine and paracrine mediators to regulate inflammation and vascular tone (21–24). In comparison, EDPs have been reported to have more potency on vasodilation and anti-inflammation than EETs (22, 24). Cumulatively, these results imply that EDPs could mediate some of the health-promoting effects of DHA. In terms of angiogenesis and cancer, EETs are

proangiogenic (25–27) and have been shown to accelerate tumor growth and metastasis by stimulation of tumor angiogenesis (28), whereas the roles of EDPs in angiogenesis and tumorigenesis have not been studied to date. To this end, we investigated the actions of EDPs on angiogenesis, tumor growth, and metastasis.

Results

EDP Inhibits Angiogenesis in Vivo. To test the actions of EDPs on angiogenesis, we chemically synthesized all stable EDP regioisomers including 7,8-, 10,11-, 13,14-, 16,17- and 19,20-EDP (4,5-EDP is chemically unstable) (22) and evaluated their effects on angiogenesis using a Matrigel plug assay in mice (29). Vascular endothelial growth factor (VEGF) is the most important regulator in pathological angiogenesis (30). Implantation of Matrigel plugs containing 100 ng VEGF in mice triggered a robust angiogenic response after 4 d of treatment. Addition of 19,20-EDP in the gel significantly inhibited VEGF-induced angiogenesis in a dose-dependent manner, with an EC₅₀ value ~0.3 μg per gel, illustrating a potent antiangiogenic effect of 19,20-EDP in vivo (Fig. 1A). We tested other EDP regioisomers and found all five regioisomers dramatically inhibited VEGF-induced angiogenesis (Fig. 1B). The 19,20-EDP also significantly inhibited fibroblast growth factor 2 (FGF-2)-induced angiogenesis (Fig. S1), demonstrating the potential broad-spectrum antiangiogenic effects of EDPs.

EDP Inhibits Angiogenesis in Vitro. Given these in vivo findings in a model system, we next studied whether EDPs have direct antiangiogenic actions on human endothelial cells. Because 19,20-EDP is the most abundant EDP regioisomer detected in vivo (16, 19), we focused on this isomer. The 19,20-EDP dramatically inhibited endothelial tube formation after a 6-h treatment in human umbilical vein endothelial cells (HUVECs), ~63% inhibition at 1 μM and ~91% inhibition at 3 μM, demonstrating its potent antiangiogenic effect in vitro (Fig. 1C). In comparison, DHA had no such effect (Fig. S2A and B). Because angiogenesis involves multiple cellular steps including endothelial cell migration, proliferation, and production of proteases (31), we studied the step at which 19,20-EDP inhibited angiogenesis. The 19,20-EDP inhibited VEGF-induced HUVEC migration on extracellular matrix (ECM) proteins fibronectin and vitronectin at a similar potency (~50% reduction at 1 μM and ~70% reduction at 3 μM, Fig. 1D

Author contributions: G.Z., D.P., M.W.K., K.W.F., and B.D.H. designed research; G.Z., D.P., L.M.M., J.Y., J.-Y.L., K.S.S.L., H.I.W., A.U., X.H., S.T., and E.S.I. performed research; K.S.S.L. and S.H.H. contributed new reagents/analytic tools; G.Z., D.P., J.Y., J.-Y.L., H.I.W., R.H.W., K.W.F., and B.D.H. analyzed data; and G.Z., D.P., J.Y., J.-Y.L., M.W.K., R.H.W., K.W.F., and B.D.H. wrote the paper.

Conflict of interest statement: University of California holds patents from the laboratory of B.D.H. on eSHI for the treatment of inflammation, hypertension, pain and other indications.

¹To whom correspondence should be addressed. E-mail: bdhammock@ucdavis.edu.

This article contains supporting information online at www.pnas.org/lookup/suppl/doi:10.1073/pnas.1304321110/-DCSupplemental.

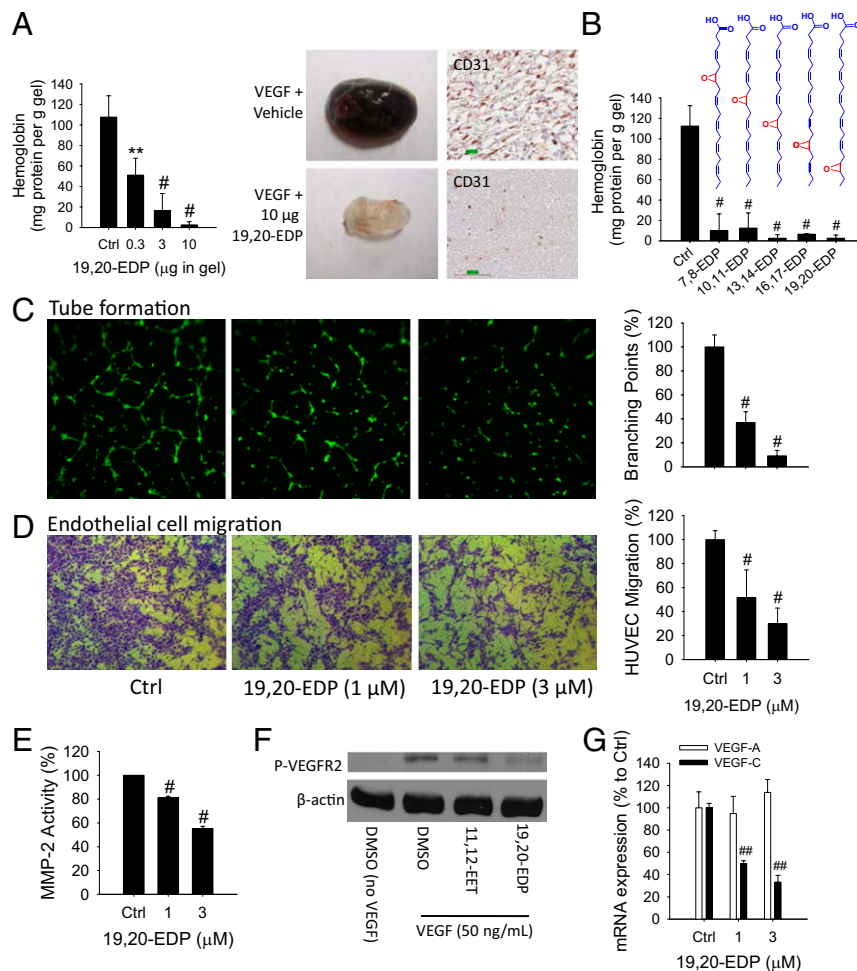


Fig. 1. EDPs inhibit angiogenesis. (A) The 19,20-EDP inhibited VEGF-induced angiogenesis in a Matrigel plug assay in C57BL/6 mice in a dose-dependent manner ($n = 4-6$ mice per group). Dose of VEGF is 100 ng per gel. (Left) Quantification of angiogenesis using hemoglobin assay. (Right) Image of representative gels and immunohistochemistry for CD31. (B) All EDP regioisomers inhibited VEGF-induced angiogenesis in mice ($n = 6-10$ mice per group). Dose of EDP regioisomer was 10 μg per gel. (C) The 19,20-EDP inhibited endothelial tube formation after 6-h treatment in HUVECs. (Left) Calcein AM-stained HUVEC microscopy. (Right) Quantification of tube formation. (D) The 19,20-EDP inhibited VEGF-induced cell migration of HUVECs on extracellular matrix protein fibronectin after 18-h treatment in HUVECs. (Left) Crystal violet-stained HUVEC microscopy. (Right) Quantification of migrated cells. (E) The 19,20-EDP inhibited MMP activity after 4-h treatment in HUVECs. (F) At a dose of 1 μM, 19,20-EDP not 14,15-EET, inhibited VEGF-induced VEGFR2 phosphorylation after 10-min treatment in HUVECs. (G) The 19,20-EDP inhibited VEGF-C mRNA expression after 6-h treatment in HUVECs. Results are presented as means \pm SD. * $P < 0.05$; ** $P < 0.01$; # $P < 0.001$; ### $P < 0.00001$.

and Fig. S2C). Endothelial cell adhesion to fibronectin and vitronectin is mediated by different integrins (32); thus this result indicates that 19,20-EDP did not target a specific integrin to suppress endothelial cell migration. The 19,20-EDP also inhibited the activity of matrix metalloproteinase 2 (MMP-2) but with a weak activity (20% reduction at 1 μM and 45% reduction at 3 μM; Fig. 1E). It had no effect on endothelial cell proliferation in HUVEC 24 h after treatment (Fig. S2D and E). In comparison, EETs such as 11,12- and 14,15-EET at 1 μM increased HUVEC proliferation by ~82% (Fig. S2E). These results support that 19,20-EDP directly targets endothelial cells to suppress angiogenesis, primarily via suppression of endothelial cell migration.

EDP Inhibits VEGF Receptor 2 Signaling. We next asked whether 19,20-EDP inhibited angiogenesis via VEGF receptor 2 (VEGFR2) signaling (30). The 19,20-EDP at 1 μM dramatically inhibited VEGF-induced phosphorylation of VEGFR2 after a 10-min treatment in HUVECs. In contrast, 14,15-EET had no such effect (Fig. 1F). We further found that 19,20-EDP inhibited VEGF expression in HUVECs. An angiogenesis array (>80 genes) suggested that among all of the proangiogenic genes, 19,20-EDP had the most

potent inhibitory effect on mRNA expression of VEGF-C (Table S1). This finding was confirmed by RT-PCR, which indicated that 19,20-EDP inhibited ~50% of VEGF-C expression at 1 μM and inhibited ~67% at 3 μM after a 6-h treatment in HUVECs, whereas it had no effect on VEGF-A expression (Fig. 1G). Together, these results indicate that 19,20-EDP inhibited angiogenesis via blocking VEGF-VEGFR2 signaling.

EDP Inhibits Primary Tumor Growth. To test the effects of EDPs on primary tumors, we studied a syngeneic Met-1 tumor, which is a highly aggressive triple-negative breast cancer (TNBC) model (33). Systematic administration of 0.05 mg·kg⁻¹·d⁻¹ 19,20-EDP (1 μg/d) by osmotic minipumps had no effect on Met-1 tumor growth after 12 d of treatment (Fig. 2A). We reasoned that this was due to the rapid metabolism of 19,20-EDP by soluble epoxide hydrolase (sEH) in vivo (22, 34-36). This was supported by LC-MS/MS analysis that the continuous infusion of 19,20-EDP did not increase its concentration in plasma and tumors (Fig. 2B). To stabilize 19,20-EDP in circulation, a low-dose selective sEH inhibitor (sEHi), *trans*-4-[4-(3-adamantan-1-yl-ureido)-cyclohexyloxy]-benzoic acid (*t*-AUCB, 1 mg·kg⁻¹·d⁻¹) (37), was coadministered with

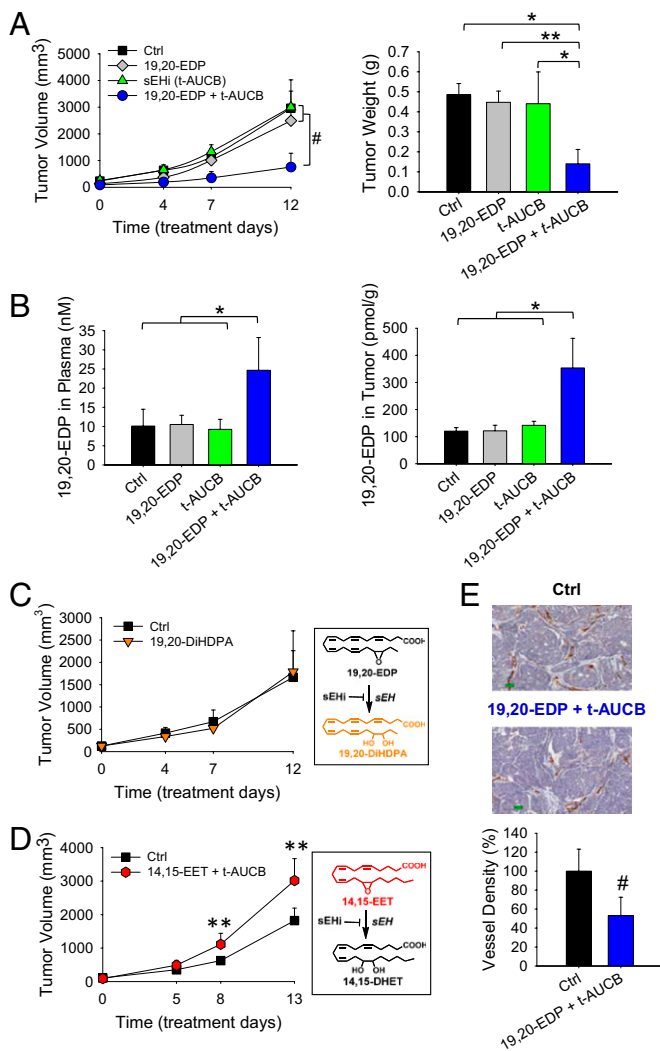


Fig. 2. EDPs inhibit primary tumor growth. (A) Coadministration of 19,20-EDP (0.05 mg·kg⁻¹·d⁻¹) and sEHi *t*-AUCB (1 mg·kg⁻¹·d⁻¹) suppressed Met-1 breast tumor growth (Ctrl: *n* = 9 mice per group; 19,20-EDP: *n* = 8; *t*-AUCB: *n* = 5; 19,20-EDP + *t*-AUCB: *n* = 11). (Left) Quantification of tumor volume. (Right) Quantification of tumor weight on day 12 of treatment. (B) Analysis of 19,20-EDP in the plasma and tumors of treated mice, coadministration of *t*-AUCB stabilized 19,20-EDP in vivo. (C) The sEH-metabolite of 19,20-EDP, 19,20-DiHDPA, had no effect on Met-1 tumor growth in mice (*n* = 4 mice per group). (Right) sEH-dependent metabolic pathway of 19,20-EDP to 19,20-DiHDPA. (D) Contrary to the effect of 19,20-EDP, coadministration of 14,15-EET (0.05 mg·kg⁻¹·d⁻¹) and sEHi *t*-AUCB (1 mg·kg⁻¹·d⁻¹) increased Met-1 tumor growth (*n* = 6–7 mice per group). (Right) sEH-dependent metabolic pathway of 14,15-EET to 14,15-DHET. (E) Coadministration of 19,20-EDP and *t*-AUCB reduced tumor vessel density, as defined by the number of CD31-positive blood vessels. (Upper) Image of representative immunohistochemistry for CD31; (Lower) Quantification of tumor vessel density (*n* = 4 mice per group). Results are presented as means ± SD. **P* < 0.05; ***P* < 0.01; #*P* < 0.001.

19,20-EDP to block the sEH-mediated metabolism. LC-MS/MS analysis confirmed that coadministration of 19,20-EDP with *t*-AUCB significantly increased the level of 19,20-EDP, from a basal level of 10.12 ± 4.38 nM to 24.67 ± 8.52 nM in plasma (*P* < 0.05) and a basal level of 120.36 ± 12.91 pmol/g to 353.4 ± 109.26 pmol/g in tumor tissues (*P* < 0.05), whereas treatment with 19,20-EDP or *t*-AUCB alone had little effect on 19,20-EDP level (Fig. 2B; complete lipid mediator profile is shown in Tables S2 and S3). With an increased level of 19,20-EDP via the combined treatment,

Met-1 tumor growth was reduced by 70 ± 20% (*P* < 0.001), whereas treatment with 19,20-EDP or *t*-AUCB alone had no effect on tumor growth (Fig. 2A and Fig. S3A–C), supporting the anticancer effect of 19,20-EDP. To further determine whether the anticancer effect is from 19,20-EDP or its sEH metabolite 19,20-dihydroxydocosapentaenoic acid (19,20-DiHDPA) (22), we tested the effect of 19,20-DiHDPA on Met-1 tumor growth. Continuous infusion of 19,20-DiHDPA (0.05 mg·kg⁻¹·d⁻¹) in mice had no effect on tumor growth (Fig. 2C), confirming the anticancer effect was not from this diol metabolite. Together, these results confirm that the combined treatment inhibited primary tumor growth via 19,20-EDP, which was stabilized by coadministration of *t*-AUCB. Contrary to the effects of 19,20-EDP, stabilized 14,15-EET increased Met-1 tumor growth by 66 ± 36% (*P* < 0.01) (Fig. 2D and Fig. S3D), demonstrating opposite effects of EETs and EDPs on tumor progression.

EDP Inhibits Tumor Angiogenesis. To determine whether the combined treatment (19,20-EDP + *t*-AUCB) inhibited tumor growth via suppressing tumor angiogenesis, we analyzed the endothelium in tumors by immunohistochemical detection of the endothelial cell marker CD31. Immunohistochemistry studies showed that the combined treatment decreased vascular density (CD31-positive vessels) by 46.8 ± 19.4% (*P* < 0.001) (Fig. 2E and Fig. S4). Cancer cell proliferation assays were carried out to test whether EDPs have direct antiproliferative effects. The 19,20-EDP at 1–3 μM had no effect on cell proliferation in multiple cancer cell lines, even when combined with *t*-AUCB to stabilize it in cancer cells (Fig. S5A). Together, these results indicate that the combined treatment inhibited tumor growth via inhibition of tumor angiogenesis, but not through a direct effect on cancer cell proliferation.

EDP Inhibits Tumor Metastasis. Tumor metastasis, the process by which tumor cells spread from the primary tumor site to other organs, causes 90% of human cancer deaths (38). Cancer cell invasion through the ECM is required to initiate tumor metastasis (38). Invasion was evaluated in vitro using a standard Matrigel-based Boyden chamber assay. With 1 μM of 16,17-EDP or 19,20-EDP, FBS-induced cancer cell invasion was reduced ~40%. Contrary to the effects of EDPs, 11,12-EET at an equal dose approximately doubled cancer cell invasion (Fig. S5B). These results suggest that EETs and EDPs may have opposite effects on metastasis.

To test the effect of EDPs on metastasis in vivo, we used a well-established Lewis lung carcinoma (LLC) model, in which resection of the primary s.c. tumor consistently stimulates growth of dormant metastases (28, 39). This spontaneous model of lung metastasis is believed to be triggered by reduced levels of circulating angiogenesis inhibitors that had been produced by the primary tumor (39) (Fig. 3A). Coadministration of either 16,17-EDP or 19,20-EDP (0.05 mg·kg⁻¹·d⁻¹) combined with *t*-AUCB (1 mg·kg⁻¹·d⁻¹) dramatically inhibited LLC metastasis, with a ~70% reduction of lung metastasis foci and lung weight (*P* < 0.001) (Fig. 3B). Surprisingly, 16,17-EDP alone significantly suppressed LLC metastasis by ~42% at day 17 after administration (*P* = 0.017) (Fig. 3B). In comparison, our previous study in the same model showed that systematic administration of 14,15-EET (0.015 mg·kg⁻¹·d⁻¹) caused an approximately three-fold increase of LLC metastasis (28), confirming the opposite effects of EDPs and EETs on tumor metastasis.

Discussion

The central finding of this study is that the DHA-derived lipid mediators EDPs inhibit angiogenesis, primary tumor growth, and metastasis. To the best of our knowledge, EDPs are unique lipid mediators to be discovered with such potent antiangiogenic, anticancer, and antimetastatic effects. In contrast, ARA-derived EETs increased angiogenesis and tumor progression, which is

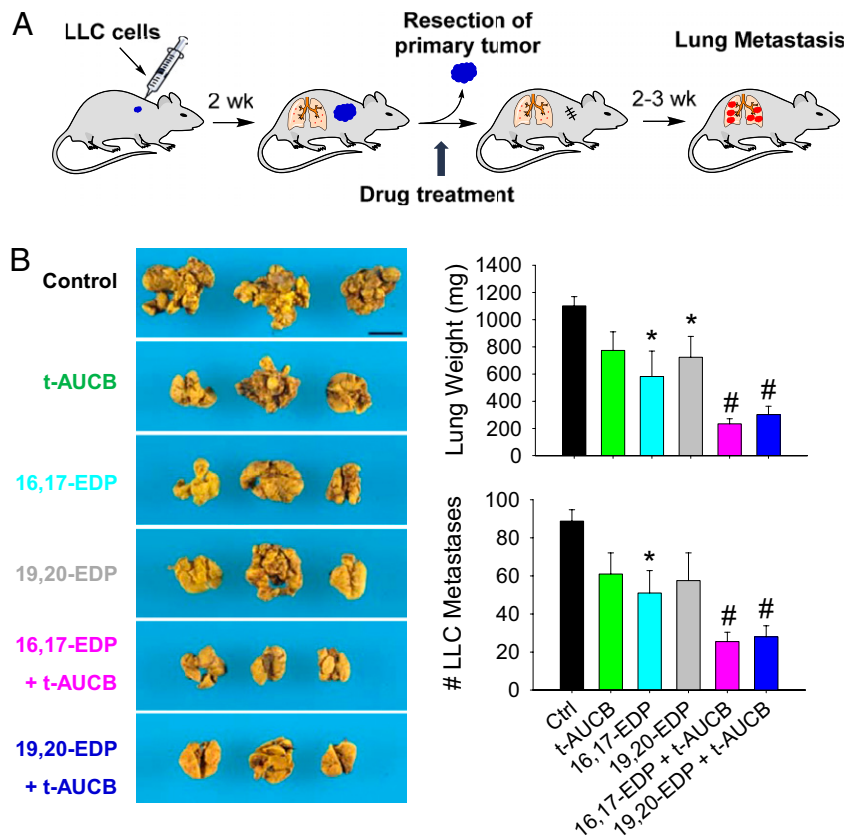


Fig. 3. EDPs inhibit tumor metastasis. (A) Lewis lung carcinoma (LLC) metastasis model in C57BL/6 mice. (B) Spontaneous LLC metastasis was decreased in EDP- and t-AUCB-treated mice relative to vehicle treatment 17 d after primary tumor removal (LLC resection). Images show representative lung metastasis in treated and control mice. (Scale bar, 1 cm.) $n = 4-5$ mice per group. Results are presented as means \pm SEM. * $P < 0.05$; # $P < 0.001$.

consistent with previous reports (26, 28). Together, these results designate EDPs and EETs as unique mediators of an angiogenic switch to regulate tumorigenesis.

Previous research of omega-3 lipid signaling has mainly focused on the COX and LOX pathways (10–13), whereas the CYP pathway, which is the third branch of the lipid metabolic cascade (14–16), has received little attention (40). The present study implies that the previously unappreciated CYP epoxygenase pathway could play a critical role in mediating the opposite effects of omega-3 and omega-6 polyunsaturated fatty acids on angiogenesis and cancer. Omega-3 fatty acids have been shown to be poor substrates of COX and LOX enzymes (17), whereas they are highly efficient alternative substrates for numerous isoforms of CYP epoxygenases (16). Supplementation of DHA in vivo reduces the levels of EETs and increases the levels of EDPs in most organs (16). Thus, an exchange of proangiogenic EETs with antiangiogenic and anticancer EDPs could explain the antiangiogenic and anticancer effects of DHA. Increased formation of EDPs has also been observed in humans upon DHA supplementation (19, 20), suggesting our findings may also be correlated with the effects of DHA in humans.

EETs and EDPs are best described as regulators of inflammation and vascular tone (21–24). Compared with EETs, EDPs are more potent than the EETs for vasodilation (~1,000 times more potent than EETs) (24) and anti-inflammation (22). These results further argue that a replacement of EETs with EDPs upon omega-3 supplementation causes multiple beneficial effects. Previous studies showed that EETs stimulate angiogenesis via up-regulation of VEGF (VEGF-A) in vitro and in vivo (25, 28). Here we found that EDP had no effect on VEGF-A expression, whereas it potently inhibited the expression of VEGF-C in vitro (Fig. 1G

and Table S1). VEGF-C is a critical mediator of lymphangiogenesis (41) and is an important therapeutic target for cancer. Currently an anti-VEGF-C monoclonal antibody VGX-100 is in phase I cancer clinical trials. Further studies are needed to test whether EDP suppresses VEGF-C and the resulting lymphangiogenesis in vivo. In addition, we demonstrate VEGFR2 as a potential cellular target for the antiangiogenic effect of EDPs. A 10-min treatment of 1 μ M 19,20-EDP dramatically inhibited VEGF-induced VEGFR2 phosphorylation in endothelial cells (Fig. 1F), supporting 19,20-EDP inhibition of angiogenesis via a VEGFR2-dependent mechanism. This is consistent with our findings that 19,20-EDP inhibited VEGF-induced angiogenesis in vitro and in vivo (Fig. 1). VEGFR2 is the most important VEGF receptor, mediating almost all known cellular responses of VEGF and is the therapeutic target of numerous angiogenesis inhibitors on the market (30). However, a common side effect of angiogenesis inhibitors that target the VEGF-VEGFR2 pathway is the induction of hypertension (42). Due to the extremely potent vasodilatory effects of EDPs (24), EDPs may have unique advantages in antiangiogenic cancer therapy by avoiding hypertension, which is a side effect associated with all current antiangiogenic drugs. Further studies are needed to investigate the effects of EDPs on blood pressure and other cardiovascular functions.

The tissue levels of endogenous EETs and EDPs are determined by the ARA and DHA released from membrane phospholipids, CYP epoxygenases, and sEH. Among the most abundant epoxy lipid mediators in omega-6 fatty acid-rich and omega-3-rich tissues are EETs and EDPs, respectively, which are further increased by genetic deletion or pharmacological inhibition of sEH (16, 43). For example, in zebrafish, 19,20-EDP was reported to be the most abundant epoxy lipid mediator; the other epoxy

lipids were very minor, and inhibition of sEH caused an approximately fivefold increase of 19,20-EDP level (43). The findings in this paper suggest that inhibition of sEH will cause opposite effects on angiogenesis in omega-6-rich and omega-3-rich tissues. Indeed, sEH inhibition increased angiogenesis in omega-6-rich tissues or cells (27, 28), whereas it suppressed angiogenesis in omega-3-rich tissues such as zebrafish and the retina (43, 44). These conflicting results can at least partially be explained by our findings of the opposite effects of EETs and EDPs on angiogenesis. Our findings further indicate that sEH could be a potential therapeutic target to treat retinal neovascularization, which is a major cause of blindness in humans (4). DHA is most enriched in retinal tissues, comprising ~60% of polyunsaturated fatty acids in retina (18). Based on our findings here, inhibition of sEH would stabilize and increase the levels of DHA-derived EDPs, attenuating retinal angiogenesis (44). Further studies are needed to test the effect of sEH inhibitors on retinal neovascularization.

A significant finding of this paper is that high levels of systemic EDPs cause dramatic inhibition of primary tumor growth and tumor metastasis by inhibiting tumor angiogenesis (Figs. 2 and 3). Based on the potent anticancer and antimetastatic effects of EDPs, EDPs are potential structural targets to develop stable analogs that mimic EDPs as anticancer agents. Previous studies have shown that fatty acid epoxides are highly unstable in vivo (34). A major pathway to metabolize the epoxides involves the sEH enzyme to generate fatty acid diols, which are usually less active (35, 36). The sEH enzyme is abundantly expressed in numerous tissues (45) and we have shown that EDPs are highly efficient substrates for sEH (22). Therefore, coadministration of a low-dose sEHi was required to stabilize EDPs in circulation, leading to dramatic inhibition of tumor growth and metastasis (Figs. 2 and 3). In the present study, administration of sEHi *t*-AUCB (1 mg·kg⁻¹·d⁻¹) had no effect on tumor growth and metastasis (Figs. 2*A* and 3*B*), and our previous study showed that *t*-AUCB at 10 mg·kg⁻¹·d⁻¹ significantly increased tumor progression (28). These results suggest that the effect of sEHi (or EETs) on tumor progression is dose dependent; more studies are needed to characterize the threshold for the effects of sEHi (or EETs) on cancer.

CYP epoxygenases such as CYP2J2 have been reported to be highly expressed in some human tumors (46). CYP3A4, which is expressed in ~80% of breast cancer and correlated with decreased overall survival in breast cancer (47), was recently identified as an epoxygenase that catalyzes the conversion of ARA to EETs (48). Overexpression of CYP epoxygenases in cancer cells or endothelial cells accelerates tumor growth and metastasis (28, 46, 49), which are largely attributed to ARA-derived EETs (18). Based on our findings, coadministration of DHA and sEHi may be an effective strategy to reduce risks of cancers with high CYP epoxygenase expression, by not only suppressing EETs but also increasing EDPs. Some anticancer drugs on the market, such as Sorafenib, are also potent sEH inhibitors (50). Analyzing the levels of EETs and EDPs in plasma or tumors, or the expression of CYP epoxygenases in tumor samples, may help to screen the patients who will most likely benefit from the omega-3 intervention.

Together, the present study and our previous report (28) demonstrate a central role of EDPs and EETs in angiogenesis and tumorigenesis, demonstrating that the CYP/sEH pathway

plays a critical role in mediating the antiangiogenic and anticancer effects of omega-3 fatty acids (4, 9). These findings also illustrate unique opportunities to treat pathological angiogenesis and cancers using omega-3 lipids.

Materials and Methods

Details of the experimental protocols are given in the *SI Materials and Methods*.

Matrigel Plug Assay. All procedures and animal care were performed in accordance with the protocols approved by the Institutional Animal Care and Use Committee of the University of California. Briefly, 0.5 mL growth-factor-reduced Matrigel (BD Biosciences) was mixed with 100 ng mouse VEGF 164 or 500 ng mouse FGF-2 (R&D Systems), 20 units heparin (APP Pharmaceuticals), with or without EDPs. Then the gel was s.c. injected into C57BL/6 mice in the abdominal area. After 4 d, the animals were euthanized to dissect the implanted Matrigel plugs. The gel plugs were weighed, homogenized in 1 mL PBS buffer, and centrifuged; the content of hemoglobin in the supernatant was analyzed by Drabkin's reagent (Sigma-Aldrich) and normalized to the gel weights. Angiogenesis was also characterized by immunohistochemistry of CD31 staining (29).

Primary Tumor Growth. Met-1 tumor pieces (1 mm³) were transplanted into the fourth inguinal mammary fat pads of FVB female mice (Charles River) (33). All of the mice in the tumor experiments were maintained on a standard mouse chow, which contains ~1.2% (wt/wt) omega-6 and ~0.2% omega-3 fatty acids. When the tumors reached the size of 2–3 mm in diameter (takes around 2 wk), the mice were s.c. implanted with Alzet osmotic minipumps (model 1002) loaded with 19,20-EDP and sEHi *t*-AUCB, which was dissolved in a mixed solvent of polyethylene glycol 400 (PEG400; 50%, vol/vol) and DMSO (50%, vol/vol). The dose of 19,20-EDP was 0.05 mg·kg⁻¹·d⁻¹ and the dose of *t*-AUCB was 1 mg·kg⁻¹·d⁻¹. During this period, animals were checked by ultrasound imaging (Acuson Sequoia 512; Siemens) to mark changes in tumor growth. At the end of the experiment, the tumors were dissected to measure tumor weight. The plasma and tumors were also collected for lipidomics analysis as described below (51). Tumor angiogenesis was analyzed by immunohistochemistry using CD31 and H&E staining.

Tumor Metastasis. Tumor metastasis was studied using an LLC model as described before (28, 39). Briefly, 14 d after s.c. injection of the LLC cells into C57BL/6 mice, the primary LLC tumors were resected to trigger spontaneous lung metastasis. On the same day of tumor resection, the mice were implanted with Alzet osmotic minipumps loaded with *t*-AUCB and 16,17- or 19,20-EDP, which was dissolved in a mixed solvent of PEG400 (50%, vol/vol) and DMSO (50%, vol/vol). The dose of 16,17- or 19,20-EDP was 0.05 mg·kg⁻¹·d⁻¹ and the dose of *t*-AUCB was 1 mg·kg⁻¹·d⁻¹. After 17 d of treatment, the mice were euthanized to dissect the lung tissues; surface metastasis foci were counted by means of a stereomicroscope.

Statistics. Group comparisons were carried out using one-way analysis of variance or Student *t* test. *P* values less than 0.05 were considered statistically significant. For tumor metastasis, data are presented as mean ± SEM; in other experiments, data are presented as mean ± SD.

ACKNOWLEDGMENTS. We thank R. Isseroff and H. Yang for microscopy, Y. Wang for ELISA, B. Inceoglu and K. Nithipatikom for discussions, and A. Kheirloomom and J. Yang for technical assistance. We acknowledge support from R01 ES02710 and National Institute on Environmental Health Sciences Superfund P42 ES04699 (to B.D.H.); R01 CA134659, R01 CA103828, and Research Investments in the Sciences and Engineering (RISE) Program of University of California Davis (K.W.F.); R01 CA148633 (to D.P.); Stop and Shop Pediatric Brain Tumor Fund and the C. J. Buckley Pediatric Brain Tumor Fund (M.W.K.); and R01 CA135401, R01 DK082690, and the Medical Service of the US Department of Veterans' Affairs (R.H.W.). B.D.H. is a George and Judy Marcus Senior Fellow of the American Asthma Society.

- Cho E, et al. (2001) Prospective study of dietary fat and the risk of age-related macular degeneration. *Am J Clin Nutr* 73(2):209–218.
- Seddon JM, George S, Rosner B (2006) Cigarette smoking, fish consumption, omega-3 fatty acid intake, and associations with age-related macular degeneration: The US Twin Study of Age-Related Macular Degeneration. *Arch Ophthalmol* 124(7):995–1001.
- SanGiovanni JP, et al.; Age-Related Eye Disease Study Research Group (2007) The relationship of dietary lipid intake and age-related macular degeneration in a case-control study: AREDS Report No. 20. *Arch Ophthalmol* 125(5):671–679.
- Connor KM, et al. (2007) Increased dietary intake of omega-3-polyunsaturated fatty acids reduces pathological retinal angiogenesis. *Nat Med* 13(7):868–873.
- Wolk A, Larsson SC, Johansson JE, Ekman P (2006) Long-term fatty fish consumption and renal cell carcinoma incidence in women. *JAMA* 296(11):1371–1376.
- Hall MN, Chavarro JE, Lee IM, Willett WC, Ma J (2008) A 22-year prospective study of fish, n-3 fatty acid intake, and colorectal cancer risk in men. *Cancer Epidemiol Biomarkers Prev* 17(5):1136–1143.
- Brasky TM, Lampe JW, Potter JD, Patterson RE, White E (2010) Specialty supplements and breast cancer risk in the VITamins And Lifestyle (VITAL) Cohort. *Cancer Epidemiol Biomarkers Prev* 19(7):1696–1708.
- Berquin IM, et al. (2007) Modulation of prostate cancer genetic risk by omega-3 and omega-6 fatty acids. *J Clin Invest* 117(7):1866–1875.

9. Rose DP, Connolly JM (1999) Omega-3 fatty acids as cancer chemopreventive agents. *Pharmacol Ther* 83(3):217–244.
10. Szymczak M, Murray M, Petrovic N (2008) Modulation of angiogenesis by omega-3 polyunsaturated fatty acids is mediated by cyclooxygenases. *Blood* 111(7):3514–3521.
11. Bagga D, Wang L, Farias-Eisner R, Glaspy JA, Reddy ST (2003) Differential effects of prostaglandin derived from omega-6 and omega-3 polyunsaturated fatty acids on COX-2 expression and IL-6 secretion. *Proc Natl Acad Sci USA* 100(4):1751–1756.
12. Sapieha P, et al. (2011) 5-Lipoxygenase metabolite 4-HDHA is a mediator of the antiangiogenic effect of ω -3 polyunsaturated fatty acids. *Sci Transl Med* 3(69):69ra12.
13. Serhan CN, Petasis NA (2011) Resolvins and protectins in inflammation resolution. *Chem Rev* 111(10):5922–5943.
14. Capdevila JH, Falck JR, Estabrook RW (1992) Cytochrome P450 and the arachidonate cascade. *FASEB J* 6(2):731–736.
15. Zeldin DC (2001) Epoxygenase pathways of arachidonic acid metabolism. *J Biol Chem* 276(39):36059–36062.
16. Arnold C, et al. (2010) Arachidonic acid-metabolizing cytochrome P450 enzymes are targets of omega-3 fatty acids. *J Biol Chem* 285(43):32720–32733.
17. Jump DB (2002) The biochemistry of n-3 polyunsaturated fatty acids. *J Biol Chem* 277(11):8755–8758.
18. Arterburn LM, Hall EB, Oken H (2006) Distribution, interconversion, and dose response of n-3 fatty acids in humans. *Am J Clin Nutr* 83(6, Suppl):1467S–1476S.
19. Shearer GC, Harris WS, Pedersen TL, Newman JW (2010) Detection of omega-3 oxylipins in human plasma and response to treatment with omega-3 acid ethyl esters. *J Lipid Res* 51(8):2074–2081.
20. Zivkovic A, et al. (2012) Serum oxylipin profiles in IgA nephropathy patients reflect kidney functional alterations. *Metabolomics* 8(6):1102–1113.
21. Node K, et al. (1999) Anti-inflammatory properties of cytochrome P450 epoxygenase-derived eicosanoids. *Science* 285(5431):1276–1279.
22. Morisseau C, et al. (2010) Naturally occurring monoepoxides of eicosapentaenoic acid and docosahexaenoic acid are bioactive antihyperalgesic lipids. *J Lipid Res* 51(12):3481–3490.
23. Fisslthaler B, et al. (1999) Cytochrome P450 2C is an EDHF synthase in coronary arteries. *Nature* 401(6752):493–497.
24. Ye D, et al. (2002) Cytochrome p-450 epoxygenase metabolites of docosahexaenoate potentially dilate coronary arterioles by activating large-conductance calcium-activated potassium channels. *J Pharmacol Exp Ther* 303(2):768–776.
25. Cheranov SY, et al. (2008) An essential role for SRC-activated STAT-3 in 14,15-EET-induced VEGF expression and angiogenesis. *Blood* 111(12):5581–5591.
26. Michaelis UR, Fleming I (2006) From endothelium-derived hyperpolarizing factor (EDHF) to angiogenesis: Epoxyeicosatrienoic acids (EETs) and cell signaling. *Pharmacol Ther* 111(3):584–595.
27. Pozzi A, et al. (2005) Characterization of 5,6- and 8,9-epoxyeicosatrienoic acids (5,6- and 8,9-EET) as potent in vivo angiogenic lipids. *J Biol Chem* 280(29):27138–27146.
28. Panigrahy D, et al. (2012) Epoxyeicosanoids stimulate multiorgan metastasis and tumor dormancy escape in mice. *J Clin Invest* 122(1):178–191.
29. Adini A, et al. (2009) Matrigel cytometry: A novel method for quantifying angiogenesis in vivo. *J Immunol Methods* 342(1–2):78–81.
30. Ferrara N, Gerber HP, LeCouter J (2003) The biology of VEGF and its receptors. *Nat Med* 9(6):669–676.
31. Folkman J (1995) Angiogenesis in cancer, vascular, rheumatoid and other disease. *Nat Med* 1(1):27–31.
32. Dormond O, Foletti A, Paroz C, Rüegg C (2001) NSAIDs inhibit alpha V beta 3 integrin-mediated and Cdc42/Rac-dependent endothelial-cell spreading, migration and angiogenesis. *Nat Med* 7(9):1041–1047.
33. Borowsky AD, et al. (2005) Syngeneic mouse mammary carcinoma cell lines: Two closely related cell lines with divergent metastatic behavior. *Clin Exp Metastasis* 22(1):47–59.
34. Catella F, Lawson JA, Fitzgerald DJ, FitzGerald GA (1990) Endogenous biosynthesis of arachidonic acid epoxides in humans: Increased formation in pregnancy-induced hypertension. *Proc Natl Acad Sci USA* 87(15):5893–5897.
35. Imig JD, Hammock BD (2009) Soluble epoxide hydrolase as a therapeutic target for cardiovascular diseases. *Nat Rev Drug Discov* 8(10):794–805.
36. Morisseau C, Hammock BD (2013) Impact of soluble epoxide hydrolase and epoxyeicosanoids on human health. *Annu Rev Pharmacol Toxicol* 53:37–58.
37. Hwang SH, Morisseau C, Do Z, Hammock BD (2006) Solid-phase combinatorial approach for the optimization of soluble epoxide hydrolase inhibitors. *Bioorg Med Chem Lett* 16(22):5773–5777.
38. Chaffer CL, Weinberg RA (2011) A perspective on cancer cell metastasis. *Science* 331(6024):1559–1564.
39. O'Reilly MS, et al. (1994) Angiostatin: A novel angiogenesis inhibitor that mediates the suppression of metastases by a Lewis lung carcinoma. *Cell* 79(2):315–328.
40. Panigrahy D, Kaipainen A, Greene ER, Huang S (2010) Cytochrome P450-derived eicosanoids: The neglected pathway in cancer. *Cancer Metastasis Rev* 29(4):723–735.
41. Skobe M, et al. (2001) Induction of tumor lymphangiogenesis by VEGF-C promotes breast cancer metastasis. *Nat Med* 7(2):192–198.
42. Chen HX, Cleck JN (2009) Adverse effects of anticancer agents that target the VEGF pathway. *Nat Rev Clin Oncol* 6(8):465–477.
43. Frömel T, et al. (2012) Soluble epoxide hydrolase regulates hematopoietic progenitor cell function via generation of fatty acid diols. *Proc Natl Acad Sci USA* 109(25):9995–10000.
44. Hu J, Popp R, Fleming I (2011) Genetic deletion and pharmacological inhibition of the soluble epoxide hydrolase attenuate angiogenesis in the murine retina. *Acta Physiologica* 201(Supplement 682):P045.
45. Newman JW, Morisseau C, Hammock BD (2005) Epoxide hydrolases: Their roles and interactions with lipid metabolism. *Prog Lipid Res* 44(1):1–51.
46. Jiang J-G, et al. (2005) Cytochrome P450 2J2 promotes the neoplastic phenotype of carcinoma cells and is up-regulated in human tumors. *Cancer Res* 65(11):4707–4715.
47. Murray GI, Patimalla S, Stewart KN, Miller ID, Heys SD (2010) Profiling the expression of cytochrome P450 in breast cancer. *Histopathology* 57(2):202–211.
48. Mitra R, et al. (2011) CYP3A4 mediates growth of estrogen receptor-positive breast cancer cells in part by inducing nuclear translocation of phospho-Stat3 through biosynthesis of (\pm)-14,15-epoxyeicosatrienoic acid (EET). *J Biol Chem* 286(20):17543–17559.
49. Jiang J-G, et al. (2007) Cytochrome p450 epoxygenase promotes human cancer metastasis. *Cancer Res* 67(14):6665–6674.
50. Liu JY, et al. (2009) Sorafenib has soluble epoxide hydrolase inhibitory activity, which contributes to its effect profile in vivo. *Mol Cancer Ther* 8(8):2193–2203.
51. Yang J, Schmelzer K, Georgi K, Hammock BD (2009) Quantitative profiling method for oxylipin metabolome by liquid chromatography electrospray ionization tandem mass spectrometry. *Anal Chem* 81(19):8085–8093.